ARMA 21–1928

Stress-Measurement Campaign in Scientific Deep Boreholes: from Planning to Interpretation

Desroches, J.
Rocks Expert, St Maime, France
Peyret, E., Gisolf, A., Wilcox, A., Di Giovanni, M., and Schram de Jong, A.
Schlumberger, Bucharest, Romania
Milos, B. Gonus, J. and Bailey, E.
Geneva Petroleum Consultants International, Geneva, Switzerland
Sepehri, S.
Independent
Garitte, B., Garrard, R. and Giger, S.
Nagra, Wettingen, Switzerland

ABSTRACT: Three candidate sites for a deep geological repository are currently being explored in Northern Switzerland. The exploration program involves drilling of at least two deep boreholes per site. A very dense stress test campaign (circa 20 stress tests per borehole) is being undertaken with a wireline formation testing tool. A detailed planning process has been developed to maximize the success rate and the coverage of stress test stations, integrating all available information as it becomes available. A dedicated stress testing protocol was also developed to ensure the most robust estimate of the stress. Improvements in the toolstring were introduced step by step to enable 100% coverage of the desired lithological column. For example, this is the first time that a single toolstring with three packers has been run to perform the complete combination of sleeve fracturing, hydraulic fracturing and sleeve reopening tests. Preliminary comparison between the stress estimates for the first two boreholes are presented.

1. INTRODUCTION

To provide the basis for site evaluation and the safety case for deep geological repositories for radioactive waste, the Swiss Cooperative for the Disposal of Radioactive Waste (Nagra) is currently drilling a series of deep boreholes in Northern Switzerland. The three sites are located 10 to 20 km apart (see Fig. 1).

The program calls for the drilling, coring, and logging of at least two new scientific deep vertical boreholes in each site. It also comprises detailed laboratory testing on core samples as well as large scale in-situ hydrological tests. The aim of the program is to provide the base state from which perturbations due to the construction of a repository, as well as those from the heat generated by the waste, can be evaluated.

One of the desired results of the program is a definition of the current state of stress as detailed as possible, not only in the designated host rock (Opalinus Clay) but also above it and below it down to the basement.

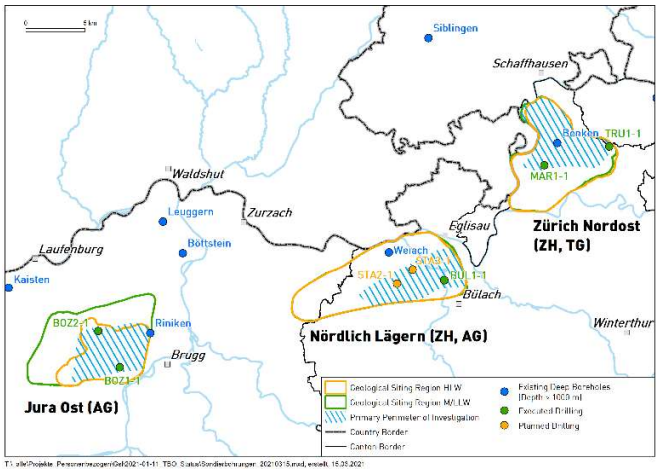

Fig. 1. Location of the three candidate sites to be assessed via the deep borehole program. Note that the drilling campaign is ongoing and that the final number of boreholes will depend on results from core analysis and in-situ testing.

A determination of the rheological parameters of the various encountered formations is also required but is outside the focus of this paper. For each site, a mechanical geomodel based on the description of the structural

geology will be populated with those rheological parameters, and tectonic boundary conditions will be tuned to match the state of stress measured in the boreholes. The model can then be used to study the long-term evolution of the site.

One of the most reliable methods to estimate the state of stress from deep boreholes revolves around the microhydraulic fracturing technique (MHF)—see Haimson and Cornet, 2003, and references within. The technique relies on the creation of a hydraulic fracture from a borehole interval sealed by inflatable packers and estimating the stress normal to the fracture surface (closure stress) from the fluid pressure in the interval. It is usually performed with a wireline-conveyed formation testing tool (e.g., Thiercelin et al., 1996). Over the last 50 years, the MHF technique has been extended from its early developments, both in terms of the existing hardware, of the protocol to estimate the closure stress, the development of supplemental tests (e.g., the opening of preexisting fractures, a.k.a. HTPF, see e.g., Cornet and Valette, 1984, the dry reopening of the created fracture, also called sleeve reopening, see e.g., Desroches, 1995), as well as interfacing it with other sources of information about the stress field (image logs, overcoring tests, convergence tests, focal mechanisms, and more). With the MHF technique as the backbone, in combination with complementary techniques, information about the complete stress tensor as a function of depth can be prized out, from ordering of the principal stresses, orientation and magnitude of the minimum principal stress to the ratio of principal stress magnitudes. Wileveau et al. (2007) and Ask et al. (2009) describe such integrated studies and their results for underground laboratories with requirements similar to those of Nagra.

Building a mechanical geomodel requires going back and forth with data acquired at different scales, from that of the core plug (centimeters), of logs (decimeters), of stress measurements with the MHF technique (meters) to the deca-kilometer geological structure. In this paper, we first report on the design process that has been developed to ensure that the location of the stress tests synchronizes with as many sources of information as possible.

A dedicated stress testing protocol, based on improvements in the stress testing tool and adjusted in real time to enable successful stress testing of a wide range of formations with differing stress regimes is presented.

Initial results are then reported, and lessons learned discussed.

2. STATION SELECTION PROCESS

A typical lithological column of the three sites is presented in Fig. 2 (from Nagra, 2021a). The target formation is the Opalinus Clay, the designated host rock for a future repository. It is part of a mostly calcareous series, with limestones and marlstones located above it and an alternance of limestones, marlstones, dolostones and evaporites below. The basement consists in regionally widespread sandstones (Buntsandstein and Rotliegend) or granite migmatites of the crystalline basement. The top of the series is Tertiary Molasse (USM).

Estimating the state of stress is desired from the top of the Malm section (in the strong "Felsenkalke and Massenkalk" limestones) to figure out how much of the regional stress field is supported by those layers, down to the basement, to figure out if there is any stress decoupling between the basement and the secondary formations above it. Given the breadth of information that is being acquired in the program, there is also a strong requirement of being able to compare stress information with that from other sources, from laboratory mechanical tests to the results of hydrological tests. Finally, the boreholes showed the development of drilling-induced fractures and drilling-enhanced features, as well as borehole breakouts, sometimes in the same formation, preventing the setting of packers to perform MHF testing.

A process to tailor MHF station locations as new information is made available has been developed to optimize the gathering of stress information in each drilling section and maximize the relevance of each test. The process flows continuously from long-term preparation to iterative short-term steps and is followed by real-time iterative adjustment of the tests. The complete process is outlined in the flow chart presented in Fig. 3. The planning part is first explained in detail below. Even though the process is continuous, the testing protocol and its adjustment ("Real-time adjustment—Iterative" in the flowchart) are detailed later in the paper.

2.1. Before the borehole is drilled—long-term preparation

Before a borehole is drilled, a global test plan is developed, providing an initial decision about which formations the stress testing should focus on, and how many stress points are desired in each formation, as well as which other tests a link is desirable to (e.g., hydrological tests, gas pressure threshold tests).

A priori information on the mechanical properties of the formations as well as initial stress prognosis showed very large variations from one formation to the next within the same drilling section. It is, however, desirable to select packer and pump modules in the stress testing toolstring so that their differential pressure limits are sufficient to enable a successful test in all targeted formations of a particular section (one toolstring designed per section).

Following the process reported in Bérard et al. (2019), the chance of success of breaking down the formation and propagating a hydraulic fracture is computed for each formation, using the hardware specifications of various toolstring combinations.

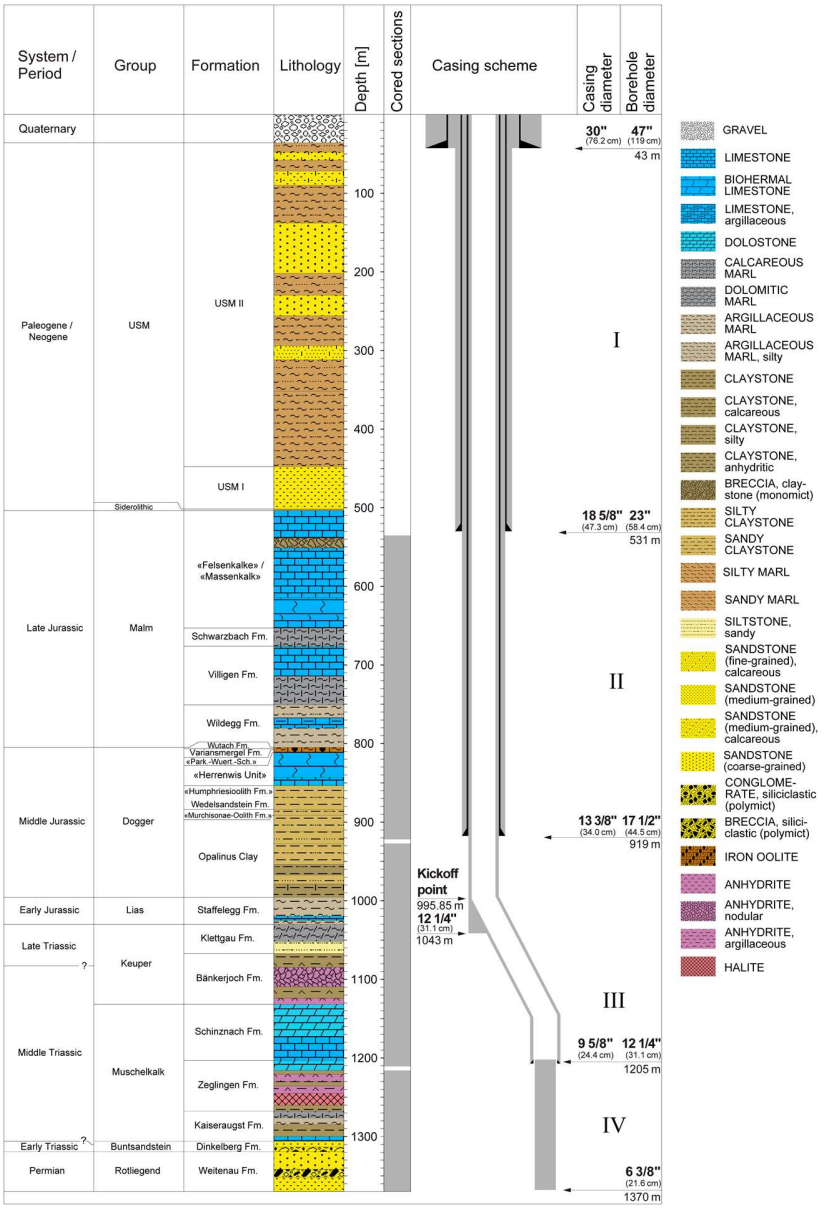

Fig. 2. Lithostratigaphic column and casing scheme for BUL1-1 borehole, Nordlich Lägern (Nagra, 2021a).

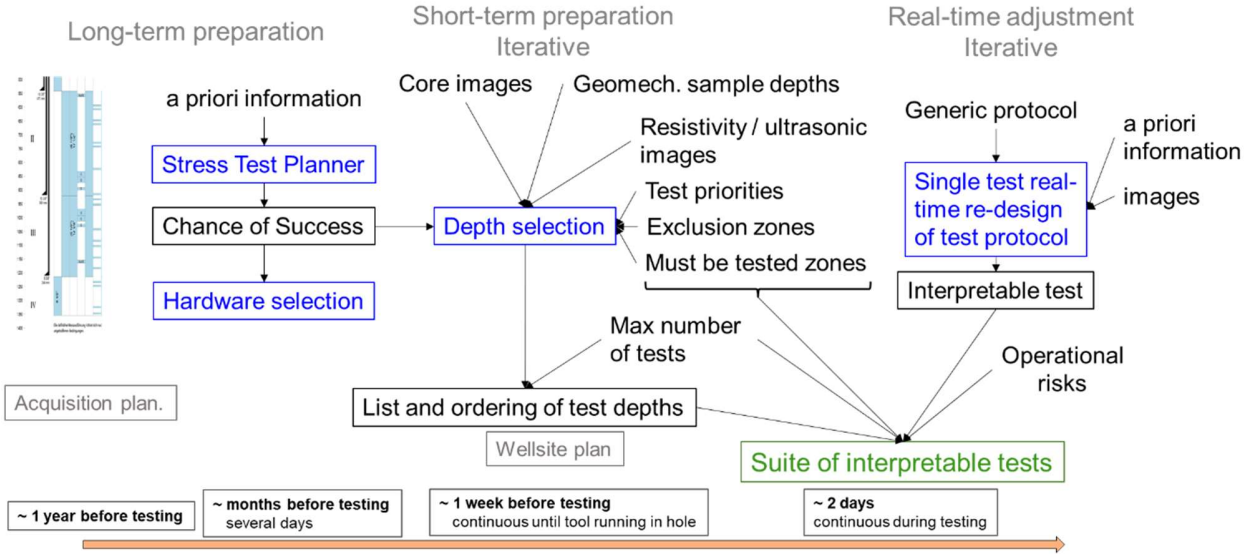

Fig. 3. Decision process for MHF testing.

From the results, a particular set of packers and downhole pump combination is selected. An example for the Bänkerjoch formation is presented in Fig. 4. The x-axis is the difference between the pressure estimated for initiating and propagating a hydraulic fracture and the maximum pressure that the tool can reach. A positive value means that the tool rating might not be sufficient. The larger the negative value, the easier fracture initiation and propagation should be. The y-axis is a probability of occurrence from 0 to 1. The colored zones are risk regions, green being risk-free, yellow corresponding to the need to be cautious (ALARP), and red meaning there is unacceptable risk to the packer. The continuous line is the probability (y-axis) of requiring a particular pressure difference larger than the value on the x-axis. For example, there is a 50% probability to require a pressure larger than about 5 MPa (~731 psi) below the tool maximum rating. The chance of success (COS) is the probability of the initiation and propagation pressure to be smaller than the maximum tool pressure. In this case, it is 89%.

Because stress test series are small—typically only a couple of points in a particular formation—one can use null hypothesis testing with the Fischer direct method (Fischer, 1934) to determine that, for a 89% COS, a minimum of two stations are required to obtain at least one successful station (within a 95% confidence level) and a minimum of three stations to obtain at least two, still with a 95% confidence interval.

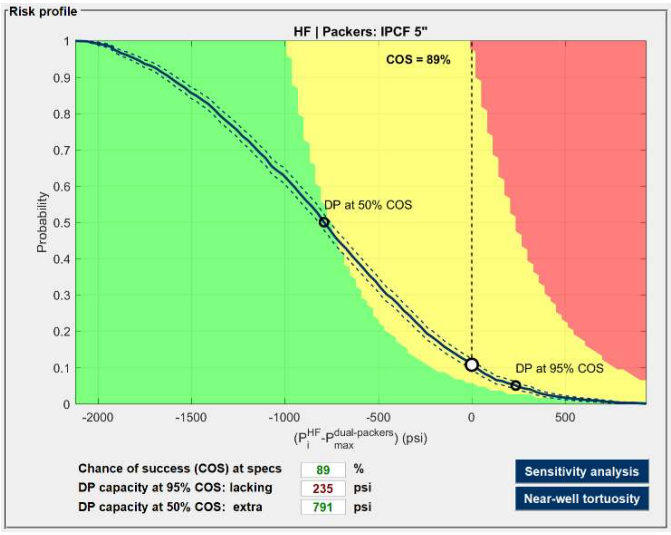

Fig. 4. Chance of success for the initiation and propagation of a hydraulic fracture in the Bänkerjoch formation in the BUL1-1 borehole.

It is thus worth checking which parameters influence the chance of success the most, to try biasing the station location towards success. In this case the ratio between the two horizontal stresses and the tensile strength of the formation are the main drivers for variance. The effect of the tensile strength can be seen in Fig. 5. The effect of a larger tensile strength becomes detrimental as soon as it is larger than about 7 MPa (~1,000 psi). Although the stress ratio cannot be known a priori, depth points with lower tensile strength are to be favored for this particular formation and this particular toolstring, for example by targeting a short preexisting longitudinal drilling induced fracture (resulting in zero tensile strength of the formation).

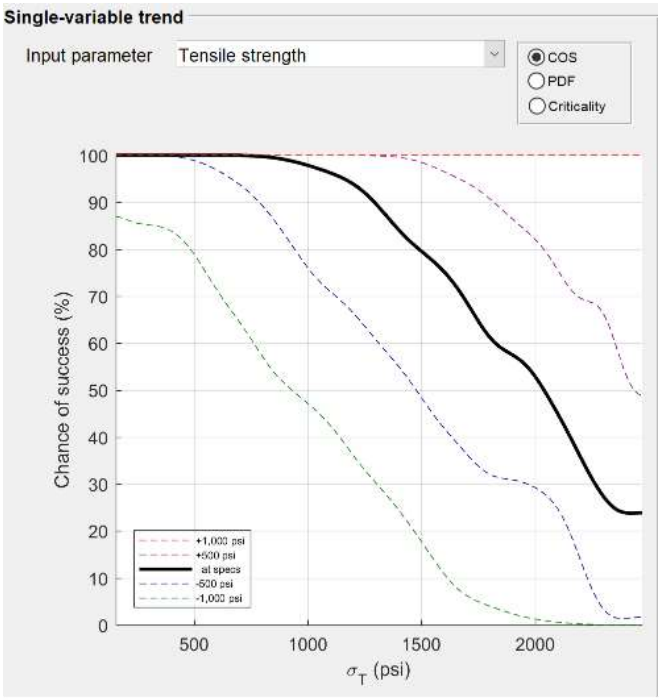

Fig. 5. Effect of tensile strength on the chance of success.

A series of short-term iterative steps is then followed, from the drilling of the borehole to the running in hole of the stress testing tool.

2.2. As the borehole is being drilled

As the borehole is being cored (with a 6 3/8-in. core barrel), core images and the location of core plugs for mechanical testing are made available. As it is desired to have stress measured at the same location as laboratory mechanical properties have been measured or, at least, close to such a location and in a similar facies, core images are being studied to reject locations with stylolites, natural fractures, or strong rock fabric at the 1-m scale that would all make the results of the stress test difficult to interpret. At this stage, the output of the process is a list of potential depths where a geomechanical sample has been taken (core interval of approximately 50 cm conditioned in resin) for further analysis, and cores don't show any issue for stress testing the formation at the corresponding location.

2.3. As the borehole is being logged

As the borehole is being logged, calipers are first analyzed. Parts of the borehole showing washouts, breakouts, or borehole closure are being removed from possible test locations. Resistivity image logs acquired

during the first logging run are then rush processed and examined for incipient breakouts, conductive natural fractures, drilling-induced fractures, and drilling-enhanced features. Unsuitable locations are again removed. As mentioned earlier, a short, focused, drilling-induced fracture is considered suitable, as it reduces the breakdown pressure and focuses the initiation of a hydraulic fracture in the interval. After this step, a number of primary locations for stress testing is prepared, together with several reserve locations in case a primary location becomes unavailable or the test at that location is not successful. If the location cannot be in front of a geomechanical sample, care is taken to select a location in a facies that is similar to one that has been sampled. The possibility to have doublets (locations in the same facies and within short distance from each other), as well as the possibility to sample all the different facies is built in that list. A risk index from 1 (negligible risk) to 3 (very high risk of test failure) is associated with each location, and the locations are ranked by order of priority in each formation.

2.4. *Before the MHF tests*

After petrophysical logging, hydrological tests to estimate hydraulic parameters of various parts of the lithological column are being run, possibly lasting several days during which the borehole is open. The final protocol that has been adopted is to enlarge the borehole to 8 1/2 in. before performing the stress tests. After the enlargement, a new series of calipers and an ultrasonic image log are being run. The state of the borehole wall is checked one last time to obtain the final list of stations. To guide the operations, the overall goal is presented, together with the minimum goal and the maximum number of stations to attempt reaching these goals. An example is presented in Fig. 6.

2.5. *During the MHF test sequence*

Based on information similar to that presented in Fig. 6, the sequence of tests is adjusted as a function of the test results and the state of the borehole. In the example outlined above, borehole stability issues were suspected in the 1,167–1,174-m interval, and the agreed strategy was to start from the top of the section. After Station 1 was successfully performed, it was not possible to go below 1,118 m. Even though the acquisition plan called for a single point in the Klettgau Formation, the decision was made to use Station 2 that had been flagged as a reserve station to cross-validate the stress in that formation.

3. STRESS TESTING PROTOCOL

Special care was taken to develop a dedicated stress protocol, as prognosis indicated that the minimum stress would be close to the vertical stress (either smaller or larger) and the boreholes are vertical.

3.1. *Alternance of single- and dual-packer tests*

The standard process utilized during the campaign alternates between single-packer and dual-packer testing as presented in Fig. 7.

First, unless the station was selected to either bracket a bed boundary that could be delaminated to create a horizontal fracture along that boundary (and measure the vertical stress) or straddle a natural fracture or a short vertical drilling induced fracture, the test sequence starts with sleeve fracturing where a single packer is inflated in front of the test interval to create a shallow pair of longitudinal fractures. The goal is to create a pair of longitudinal fractures that will focus fracture initiation and reduce the breakdown pressure (see Thiercelin et al., 1994).

Goal:
4 interpretable tests
Minimum goal:
1 interpretable test for Klettgau and for Bänkerjoch
Maximum of:
6 stations.

Ordering doesn't mean that all stations will be attempted.
Numbers with () will be attempted only if required.

Order	Formation	MHF Interval Depth (m)	MHF tool depth	Sleeve tool depth	In front of GM samples	Priority	Risk (1 /2)	Sleeve Fracturing ?
1	Klettgau	1045.4	1049.14	1053.46	Close - similar facies	1	2 (breakdown)	Y
(2)	Klettgau	1052.5	1056.24	1060.56	Close - different facies	2	2 (bottom packer); use if no breakdown achieved.	Y
3	Bänkerjoch	1121.85	1125.59	1129.91	Y	1	2 (Bed Boundaries?)	Y
4	Bänkerjoch	1125	1128.74	1133.06	N	1	2: attempt to reopen bed boundary - to differentiate between Sv and Shmin	NO, but YES for SR
(5)	Bänkerjoch	1131.2	1134.94	1139.26	N	2	2 (complex DIFs) use if no breakdown achieved	Y
6?	Schinznach - Liedertswil	1195.1	1098.84	1103.16	Y	1	2 (interpretation)	Y

Fig. 6. Operational depth selection– borehole guidance for the fourth section of the first borehole. All proposed stations had a medium risk index of 2. Sv: overburden stress. Shmin: minimum horizontal stress. SR: sleeve reopening. DIF: Drilling induced fracture.

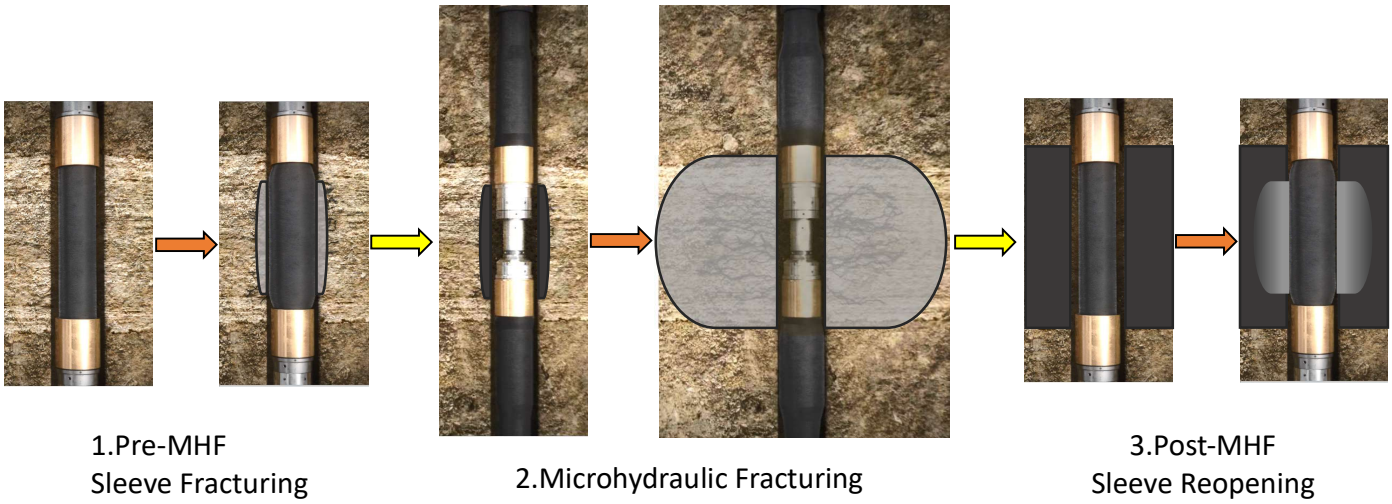

Fig. 7. Sleeve fracturing / MHF / Sleeve reopening test protocol. The toolstring is moved between step 1 and 2 so that the middle of the interval between the straddle-packer arrangement is where the middle of the single packer was. Between step 2 and 3, the tool is moved again so that the single packer is at the same depth as where it was for step 1.

Second, in all cases, the interval is straddled with a pair of packers and tested following a microhydraulic fracturing protocol that stems from a standard protocol designed for the entire stress campaign but is adjusted in real time depending on the response of the formation and will be further discussed below.

Third, if the MHF test was deemed successful, sleeve reopening is performed by inflating a single packer in front of the tested interval. The goal is to either reopen the longitudinal fracture that was created during the MHF test and obtain an estimate of the maximum horizontal stress (see Desroches and Kurkjian, 1999), or validate by the absence of a sleeve reopening signature that the longitudinal fracture initially created by sleeve fracturing was not propagated into the formation (and that a horizontal fracture was likely created).

The tests discussed throughout this paper were performed with both single and dual packers mounted on a wireline-conveyed formation testing tool. Combinations of sleeve fracturing and MHF have been run in the past in a single run with a toolstring comprising three packers (e.g., Mishra et al., 2011). This is, however, the first known example of the complete sleeve fracturing, MHF and sleeve reopening procedure being performed in a single run. More details about sleeve fracturing, as well as the hardware and the operational part of these MHF tests, are outside of the scope of this paper and can be found in Desroches et al., 2021.

3.2. MHF test protocol

The MHF technique relies on isolating an interval between straddle packers and injecting fluid into it to create and propagate a hydraulic fracture. Theoretically, such a fracture will propagate perpendicular to the minimum principal stress. The fracture width is directly linked to the difference between the fluid pressure in the fracture and the stress acting normal to the fracture surface. Detecting and measuring the fluid pressure at which the fracture width is zero provides an estimate of the stress acting normal to the fracture or closure stress.

Because the fluid pressure in the fracture is not constant (see e.g. Möri and Lecampion, 2021 for a discussion of the hydraulic fracturing process during propagation and shut-in), and the pressure is measured in the borehole, several closure pressure estimates are being collected to bracket the stress acting on the fracture surface. Upper bounds are pressure estimates taken during the fracture propagation phase: Propagation Pressure, and Instantaneous Shut-in Pressure (ISIP), which is the pressure immediately after pumping has been stopped. The pressure at which the fracture closes after injection (Closure Pressure) allows to probe the pressure corresponding to zero fracture width from the open state (detecting closure). The pressure at which the fracture reopens during injection (Reopening Pressure) allows to probe it from the closed state (detecting reopening).

Because there is a stress concentration around the borehole, the fracture surface needs to develop far enough into the formation to mostly sense the “far-field” state of stress (in the sense of being unperturbed by the presence of the borehole). However, the test doesn’t allow for a direct measurement of the fracture extension. To make sure that the tested fracture senses the far-field stress, several cycles of fracture propagation and fracture closure are performed, until one observes convergence of the various closure stress estimates from one cycle to the next. Until such convergence is achieved, it is not guaranteed that the fracture mostly senses an area of the formation that is subject to a constant stress value.

The basic building block for each cycle consists in injecting fluid at a constant rate and propagating the fracture for a certain time and volume before observing pressure decay after injection has stopped.

The toolstring that was used allows several additional building blocks that are especially useful when the formation tested is close to impermeable. In such a case, the time to wait for fracture closure can reach several hours or more, making it operationally impractical to identify the fracture closure in most cases. These additional building blocks will be briefly described below. More detail can be found in Desroches et al., 2021.

The first additional block consists in gradually increasing the injection rate in steps (step-rate test). The interpretation is solely based on the propagation of the fracture (Nolte, 1982, 1988). An example is presented in Fig. 8.

Another additional building block, the slamback-rebound test, consists in short and fast fluid withdrawal from the interval after injection has stopped and watching the fracture rebound. When properly executed, the fracture first closes only at the borehole wall and then produces back into the interval. A rebound pressure significantly larger than the borehole hydrostatic confirms the creation of a hydraulic fracture and is considered a critical QA/QC step (Thiercelin et al., 1994). The schematic of an ideal case is presented in Fig. 9. Real-life examples are part of the example detailed in Section 4.

A final building block consists in a slow withdrawal of fluid from the fracture akin to the forced closure procedure in hydraulic fracturing (see Plahn et al., 1995 for an early study and Malik et al., 2016, for a different means to perform it). It is achieved by adding a specially modified sample chamber module in the toolstring, which creates a metered connection between the interval and the mud column outside the sealed interval (see right panel of Fig. 10).

A comparison between a cycle with a regular falloff during which fracture closure was not reached after 30 minutes waiting time and a subsequent cycle with a forced closure test that closed the fracture within less than 5 minutes is presented in the left panel of Fig. 10. Note that the presence of a fracture is confirmed by a slamback-rebound test after the forced closure part of the cycle.

The test protocol (varying fluid injection rates and volumes, allowing the fracture to close unaided or forcing it to close) is tailored in real time for each test. The protocol for each subsequent cycle is based on the observation of the previous cycles. An example will be presented in Section 4.

3.3. Reconciliation plot

No single parameter (closure pressure, reopening pressure, ISIP, etc.) determined on a single hydraulic fracturing cycle is a good enough estimate for the closure stress, let alone the magnitude of the far-field minimum stress. Once each cycle has been analyzed separately, it is necessary to interpret the stress test record in its entirety to determine the best possible estimate of closure stress as well as robust lower and upper bounds. Estimates are plotted for every cycle along the time axis in a reconciliation plot (Desroches and Kurkjian, 1999) – an example is presented in Fig. 11.

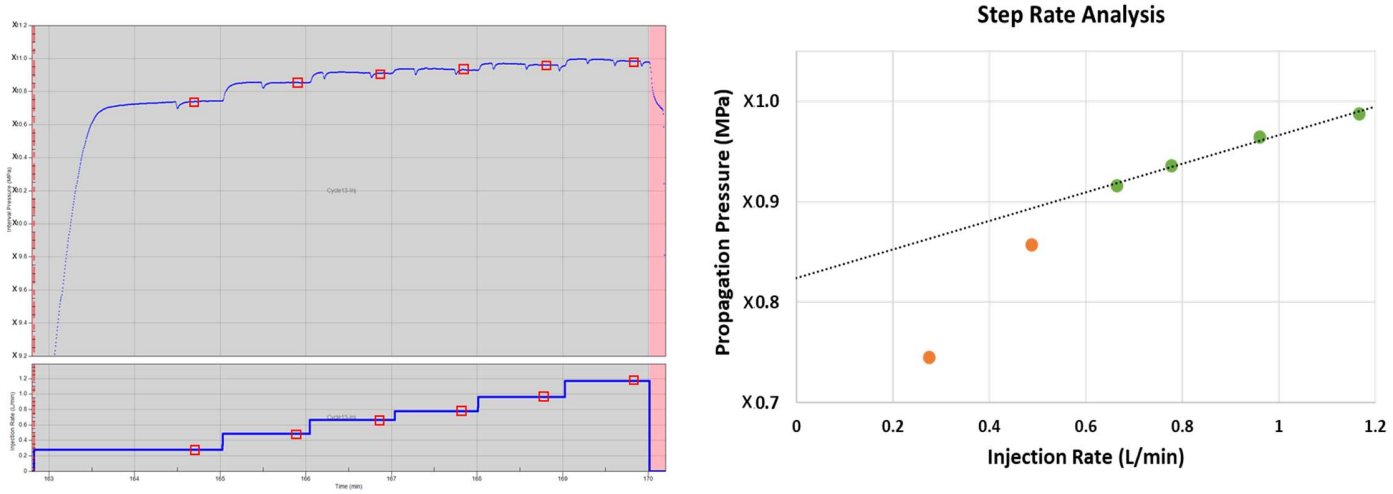

Fig. 8. Example of step-rate test and corresponding analysis. Left plot: top plot is interval pressure versus time, with points for analysis highlighted as red squares; bottom plot is corresponding injection rate as a function of time. Right plot: interval pressure versus injection rate; the fracture is considered to not be propagating for the orange points, whereas it is considered to be propagating for the green points. The zero flow-rate intercept of a best fit line going through the green points (dashed line) provides an estimate for the closure stress.

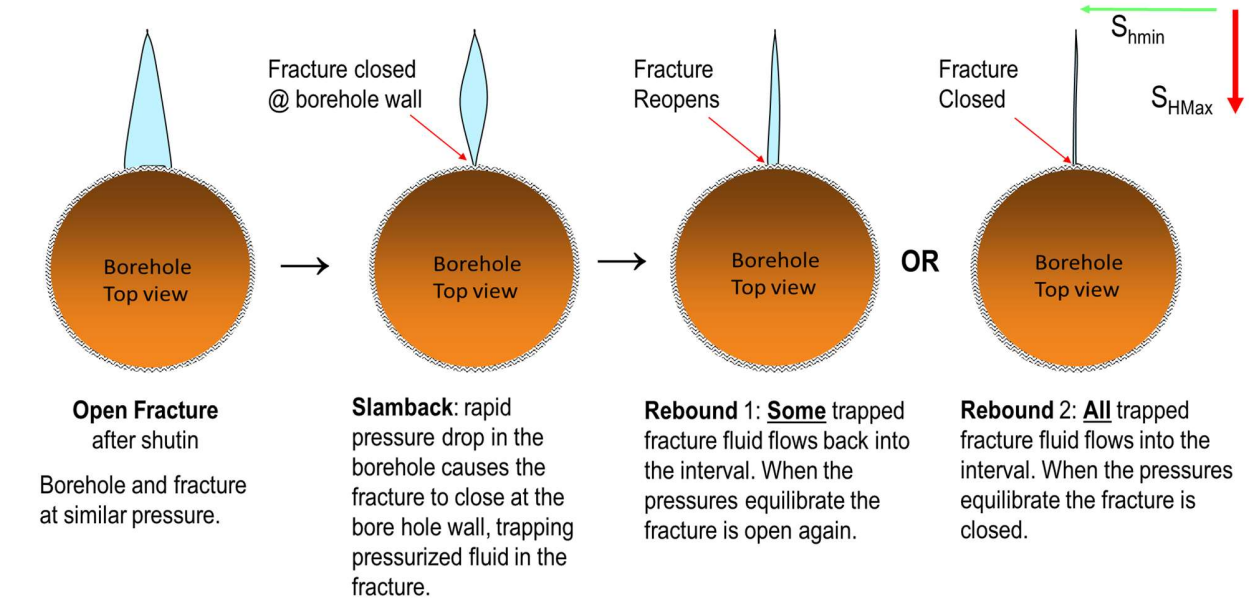

Fig. 9. Steps for slamback-rebound test.

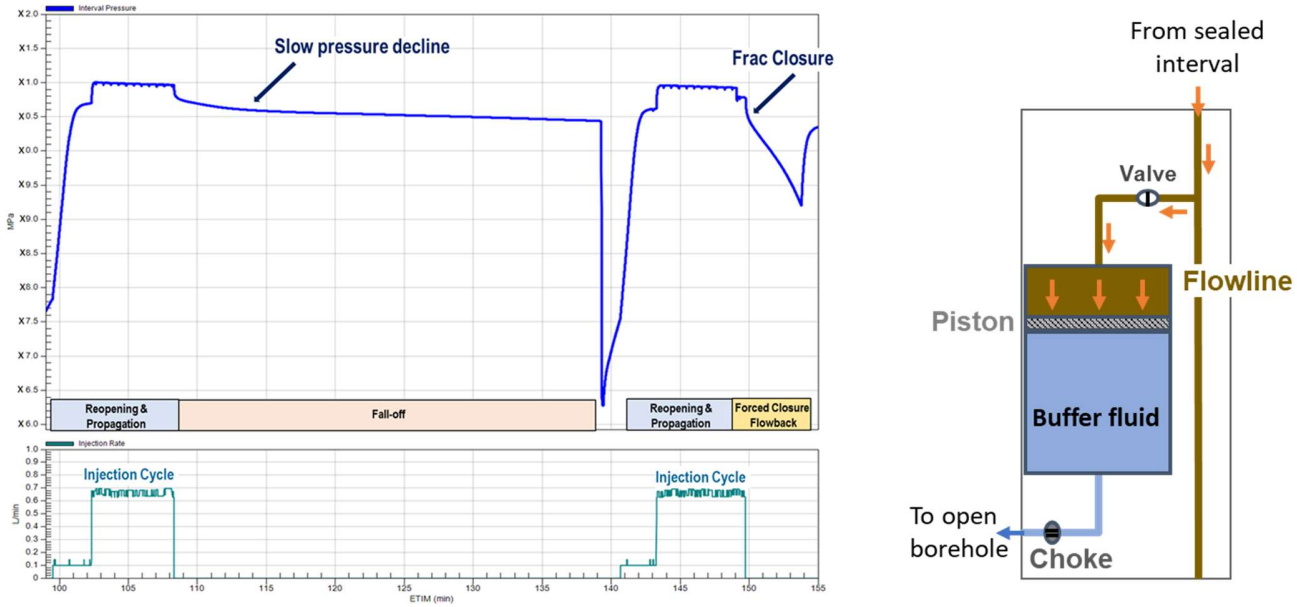

Fig. 10. Left panel: example of forced closure test, interval pressure on top and injection rate at the bottom. Right panel: schematic of the hardware behind the forced closure test.

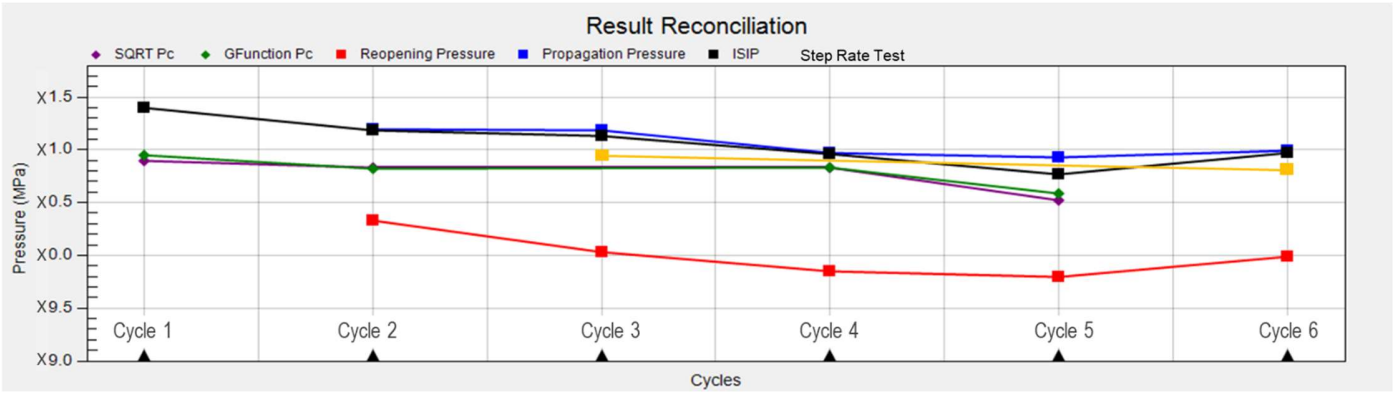

Fig. 11. Example of a reconciliation plot for a single depth where multiple cycles are plotted together to assess the consistency of the data. SQRT Pc corresponds to closure pressure determined from a square-root of shut-in time plot, GFunction PC to that determined from a G-function plot.

The reconciliation plot provides confirmation that the fracture has grown out of the influence of the wellbore. Once the fracture is mostly sensing the far-field stresses, estimates of the closure stress stop varying from one cycle to the next. If no consistency (repeating of the values for a certain parameter like closure pressure within a certain range) is found on the reconciliation plot, the data cannot be considered representative. Once convergence has been achieved, the upper bound is typically selected from the larger upper bound estimate of the converged cycles, and the lower bound typically from the lowest lower bound estimates of the converged cycles.

3.4. Example

An example of a complete pressure record with the associated reconciliation plot is presented in Fig. 12.

The top plot shows pressure in the interval and fluid injection rate as a function of time. The reconciliation plot at the bottom shows characteristic pressures estimated for all six cycles for which a fracture was created and tested (Cycle 1 to Cycle 6). ISIP stands for instantaneous shut-in pressure. Because of the use of a downhole pump, there is little frictional pressure drop and ISIP is taken as the first point after the pump has stopped. Pc stands for closure pressure and is typically determined via specialized plots of pressure against either square-root of shut-in time or G-function.

Cycle 1 shows the creation and propagation of a hydraulic fracture. Subsequent cycles show variations in the test protocol: Cycles 2, 4, and 6 are reopening tests, and Cycles 3 and 5 are step-rate tests. A slamback-rebound test was performed on cycles 1, 3, 4 and 5.

The characteristic pressures—closure stress estimates—presented in the reconciliation plot reflect the stress acting on the fracture as it is propagated. They validate the creation of a hydraulic fracture and show a clear trend towards convergence that supports that an estimate of the far-field stress can be obtained from the test.

4. REAL-TIME TAILORING OF THE TEST PROTOCOL

The same example will be used to illustrate how the test protocol is changed in real time as the test unfolds. A summary of the important steps is presented in Fig. 13. During the first cycle, the propagation pressure makes it difficult to discriminate between a stop and go fracture propagation and a high-pressure leak. A slamback-rebound test at the end of the cycle confirms a fracture was indeed created, and that the test can continue without altering the setup. After the first and the second injection cycles, there is no clear fracture closure signature, and there is still a signature akin to a breakdown at the beginning of the test, which makes fracture reopening analysis impossible.

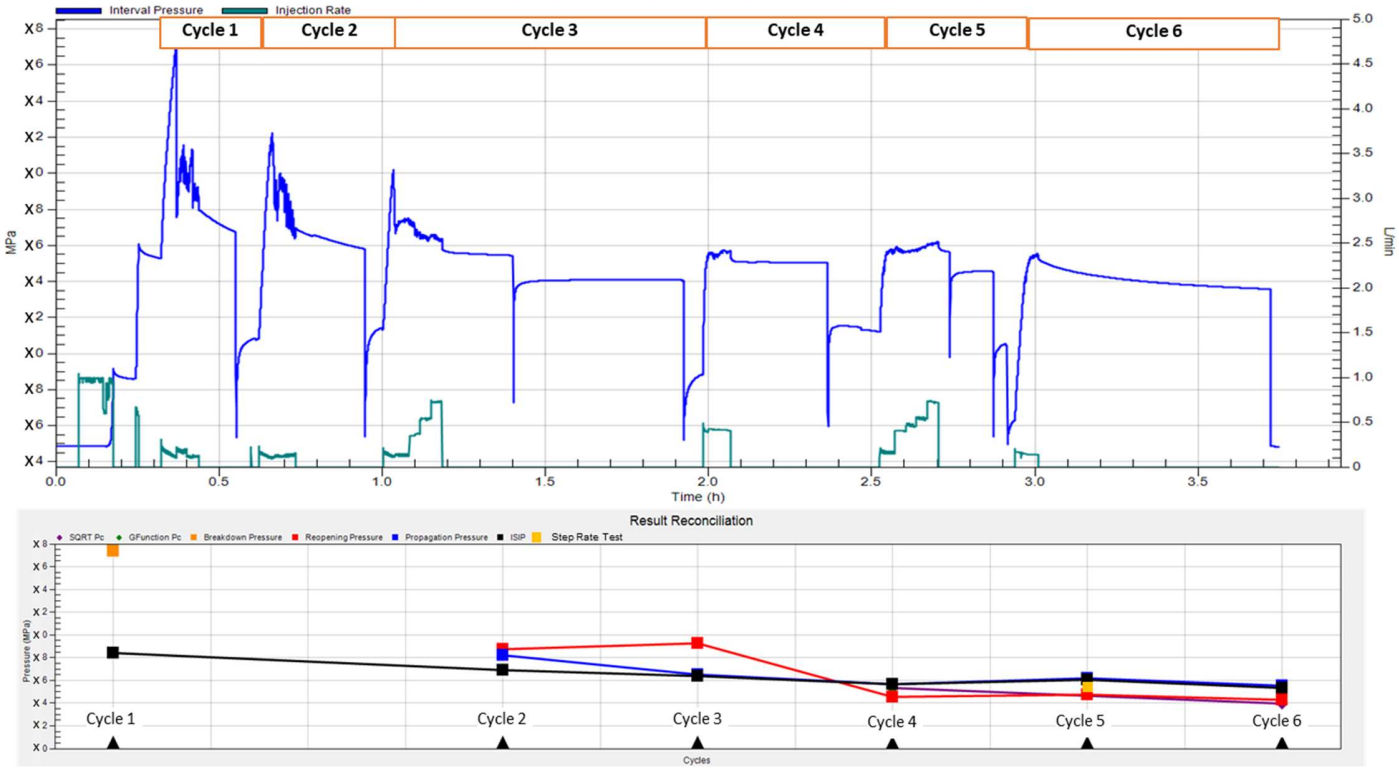

Fig. 12. Example of pressure record and associated closure stress estimates. Top panel: interval pressure vs. time. Bottom panel: reconciliation plot, where the propagation pressure and the ISIP are nearly similar.

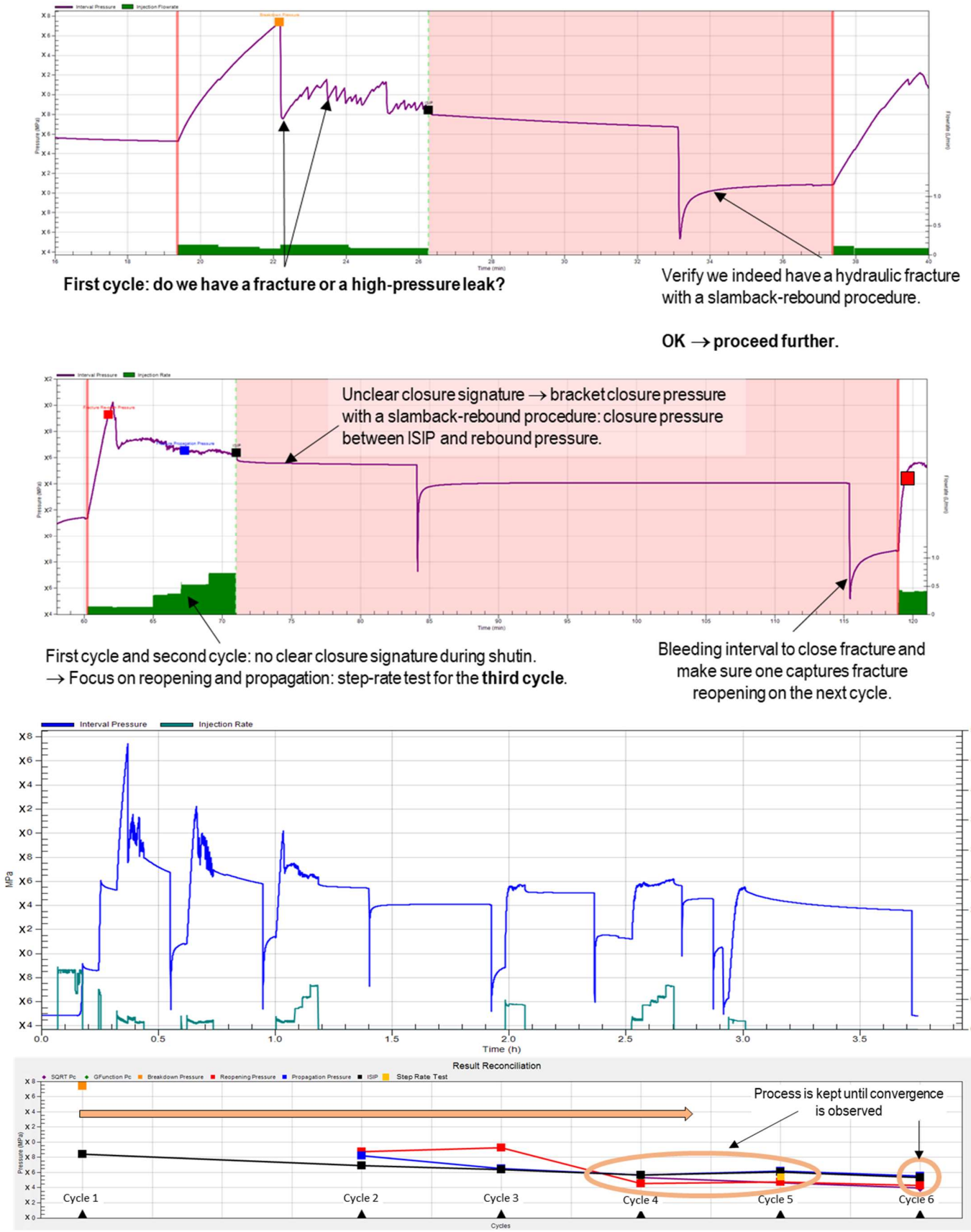

Fig. 13. Real-time tailoring of the MHF test protocol.

A step-rate test is performed during the third cycle to focus on propagation, after which the fracture closure is bracketed by a slamback-rebound test. Such a process is kept until convergence is observed (highlighted on the reconciliation plot). The test ends with a very slow reopening cycle, which provides an excellent estimate of the closure stress when the fracture is well developed. The reconciliation plot allows to determine a lower bound for the closure stress of 24.48 MPa and an upper bound of 25.5 MPa.

5. BOREHOLE IMAGE LOGS

The borehole imaging tool is then run a second time after the stress testing to evaluate if and where fractures have been created and to provide information about fracture orientation and direction for proper stress evaluation. In Fig. 14, pre- and post-MHF images are presented. New fracture traces induced by the MHF test are shown with blue arrows on the rightmost track. The trace of these fractures has been superimposed (in red) on the static pre-MHF resistivity image to show that the pre-MHF resistivity image does span the location where these new traces appear and that there were no preexisting fractures there. The MHF test led to the creation of a two-winged vertical fracture at the wellbore that spans nearly the entire length of the straddle-packer arrangement. The azimuth of these new fracture traces indicates that of the maximum horizontal stress.

6. RESULTS

A "quick-look" profile of closure stress along the lithological column and the integrated formation density is presented for the first borehole of the program in Fig. 15. Contrarily to the detailed interpretation that results in a lower bound, an upper bound and a best guess for the closure stress, the quicklook profile consists of an upper and a lower bound. Because of the goal of these stress tests, the bounds have been selected so that one is as certain as possible that the closure stress is above the lower bound and below the upper bound. This is different from classical interpretation that tries to put "reasonable" bounds, that the actual closure stress value could possibly be outside of. All closure stress values have been assigned to the minimum horizontal stress, apart from that at 767.2 m where an inclined preexisting natural fracture was tested (so that the closure stress is an upper bound for the minimum stress) and that at 668.4 m where the stress assignment is unclear (and will thus not be used further).

In Table 1, the lower and upper bound for the closure stress are being reported as a function of the formation for the first two boreholes, borehole BUL1-1 (Nagra 2021a) and borehole TRU1-1 (Nagra 2021b), respectively. To compare the values, because the formations are at different depths, the gradient has been computed and reported as specific gravity. Grayed cells indicate that no successful test was performed for that formation.

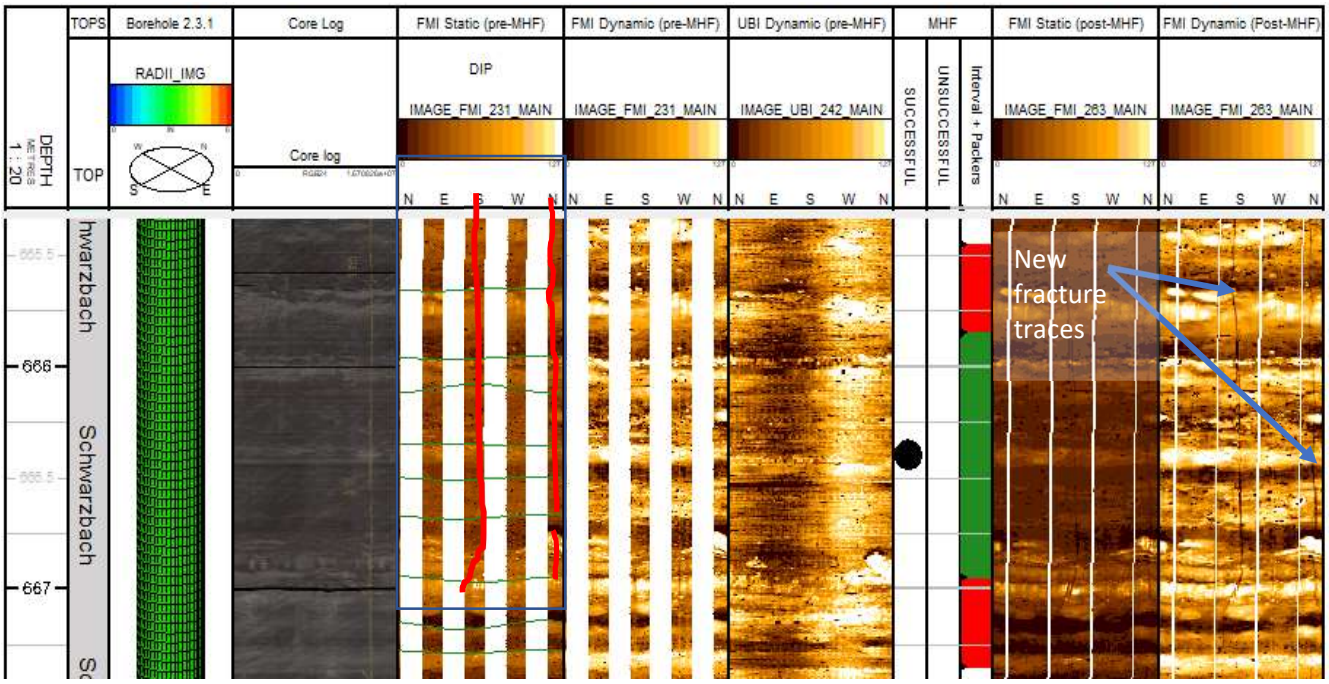

Fig. 14. Example of pre-MHF images, from left to right: depth (MD), formation name, borehole shape from ultrasonic log, core photograph, pre-MHF resistivity image log (static and dynamic image), pre-MHF ultrasonic image dynamic image; MHF location (successful/unsuccessful flag, location of packers in red, location of interval in green); post-MHF resistivity image (static and dynamic).

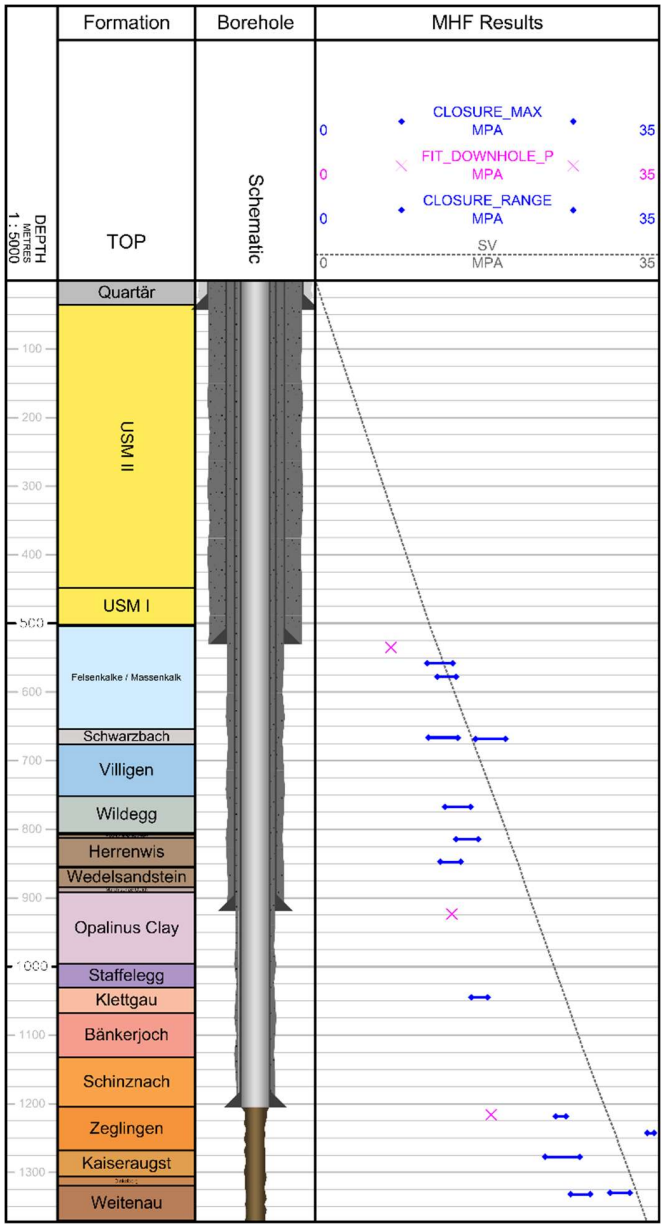

Fig. 15. Comparison of the quick-look closure stress range obtained from the MHF tests with the overburden stress from the integration of density (Sv) and the maximum pressures attained during the formation integrity tests (FIT).

Preliminary values of the closure stress suggest that, in the upper Malm (Felsenkalke/Massenkalk and Schwarzbach formations), the stress is higher in the first borehole. This is in line with information from the structural setting of the two boreholes. On the other hand, values are comparable or higher in the second borehole in the Wildegg (lower Malm) and the Klettgau formations. No clear conclusion can be drawn yet for the Opalinus Clay or the bottom of the lithological column and the results of the companion borehole of BUL1-1 will be required to further the analysis.

Development of the protocol, both for the selection of the test depth and for the real-time adjustment of the MHF test, has also shown improvement in the success rate. For both the first and the second borehole, the number of stations that were planned was respectively 40% and 50% higher than the desired number of stations in the acquisition plan. In other words, 40–50% more tests were planned than the desired number of tests. Based on the improvement of the protocols, however, the success ratio of actual tests went from 65% for the first borehole to 79% for the second one. More importantly, the ratio of successful tests to the number of desired tests went from 68% to 110%.

Table 1. Comparison of the closure stress range for the first two boreholes

Age Group	Formation	Closure stress lower bound (SG) BUL1-1	Closure stress upper bound (SG) BUL1-1	Closure stress lower bound (SG) TRU1-1	Closure stress upper bound (SG) TRU1-1
Malm	Felsenkalke / Massenkalk	2.08	2.56	1.98	2.35
		2.19	2.52	2.08	2.32
	Schwarzbach	1.76	2.22	1.53	1.88
	Villigen			1.76	1.99
				1.97	2.23
				1.77	2.07
	Wildegg	1.75	2.10	1.90	2.04
Dogger	Humphriesioolith to Murchinsonae-Oolith			1.49	2.21
				1.94	2.05
	Herrenwis	1.79	2.08		
		1.53	1.78		
	Opalinus Clay			1.77	2.23
				1.82	2.09
				2.02	2.33
				1.90	2.11
				1.29	1.76
Lias	Staffelegg				
Keuper	Klettgau	1.55	1.71	2.06	2.27
				1.92	2.19
	Bänkerjoch			2.27	2.47
				2.06	2.39
				2.42	2.81
Muschelkalk	Schinznach			1.28	1.80
				1.22	1.79
	Zeglingen	2.05	2.13		
		2.77	2.83		
		1.87	2.15		
	Kaiseraugst				
Bundsandstein	Dinkelberg			2.14	2.46
Permokarbon	Rotliegend	2.33	2.48		
		1.99	2.11		

Improvements in the drilling practice also allowed to obtain five successful tests in the target formation in the second borehole (instead of one unsuccessful test in the first borehole). Note that to mitigate such risks, boreholes are drilled in pairs, so that the absence of data in a particular formation in one borehole in one site can trigger a high-priority acquisition in the next "companion" borehole in the same site. The companion borehole to the first borehole is being drilled during the first half of 2021.

7. DISCUSSION AND CONCLUSIONS

The combination of the specific depth selection process developed here (enabled by the richness of available data), together with the specific toolstring deployed in the campaign and the real-time tailoring of the test protocol,

were crucial to successfully estimate stress profiles with a test success rate ranging from 65% to 100% and a coverage rate measured by the number of successful tests compared to the number of initially desired tests, of 67% to 125%.

This is the first time that the complete sleeve fracturing, microhydraulic fracturing, and sleeve reopening for stress testing procedure has been performed using a single, three-packer toolstring, making such a process a lot easier to run.

The program has called for a continuous tuning of the tool hardware to be able to reduce the number of formations where no stress test could be performed. In particular, the toolstring that was used for the second borehole did not allow the estimation of stresses in the Zeglingen evaporites section. An upgrade of the sleeve fracturing packer to one with a higher (80 MPa) differential pressure rating similar to that reported in Povstyanova et al. (2018) enabled stress testing there in subsequent boreholes.

Other tool hardware modifications introduced during the course of the program (upgrade of the downhole pump and adding the possibility for forced closure) allowed to significantly decrease the range of the closure stress determination (whilst keeping the same stringent requirements on the lower and upper bound determination). For example, the difference between the upper and the lower bound in the target formation improved from 1.8–4.2 MPa in the second borehole to 0.3–2.0 MPa in the fourth borehole. Note that further interpretation can shrink this range further, though this hasn't been completed for all boreholes yet.

Regardless of how much care is being taken to core the boreholes, the imaging logs prior to the stress tests are proving key to the test depth selection. The various decisions could not be adequately taken with cores, calipers, or sonic logs alone.

Because the magnitude of the overburden and that of the minimum horizontal stress are close in parts of the lithological column, the comparison between imaging logs before and after the test, coupled to the reconciliation plot to resolve any possible fracture reorientation, are also proving to be necessary for assigning the closure stress value to the vertical or the horizontal stress direction.

The campaign mentioned in this paper will result in a unique dataset. At the time of preparing this paper, five boreholes drilled in the very same lithological column have been completed, with 124 MHF stations, and 164 sleeve fracturing and sleeve reopening stations performed, with at least two additional boreholes to be tested. These will provide a unique sample of the lateral variability of stresses at the deca-kilometer scale. Furthermore, inversion of the tests via a hydraulic fracturing model (e.g., Desroches and Thiercelin, 1993) will provide a comparison of the plane strain Young's modulus at the scale of the MHF test with other values of the same modulus measured at different scales, strains, and frequencies but at the same location, providing more insight into the comparison of such measurements. Interpretation of drilling induced fractures, when they are present, could also be compared with results of the stress measurement campaign, further validating the interpretation methodology of such features (e.g., Nelson et al., 2005).

Finally, the results of the stress measurements are being used to calibrate and update existing 3D mechanical geomodels (Hergert et al., 2015), and validate or invalidate the original hypotheses that were made on the tectonic boundary conditions. Preliminary analyses indicate that tectonic shortening might be less severe than previously envisaged, changing the predictions in the entire modeled area. Updated with new structural information, mechanical properties, and stress measurements, these calibrated models will prove crucial to evaluate the response of the different sites to the excavation of a repository and to the thermal loading from the stored material.

ACKNOWLEDGMENTS

Permission from Nagra and Schlumberger to publish this work is gracefully acknowledged.

GPCI authors wish to thank Emerson Paradigm for their support.

REFERENCES

1. Ask, D., O. Stephansson, F.H. Cornet, and M.-V.-S. Ask. 2009. Rock stress, rock stress measurements, and the integrated stress determination method (ISDM). *Rock Mechanics and Rock Engineering* 42(4), 559–584
2. Bérard, T., N. Chugunov, J. Desroches, and R. Prioul. 2019. Feasibility and Design of Hydraulic Fracturing Stress Tests Using a Quantitative Risk Assessment and Control Approach. *Petrophysics* 60(1):113-135.
3. Cornet, F.H., and B. Valette. 1984. In situ stress determination from hydraulic injection test data, *J. Geophys. Res.*, 89(B13), 11527– 11537.
4. Desroches, J. & M. Thiercelin. 1993. Modelling the propagation and closure of micro-hydraulic fractures. *International Journal Rock Mechanics and Mining Sciences*, 43(7), 1231-1234.
5. Desroches, J. 1995. Stress testing with the micro-hydraulic fracturing technique: Focus on fracture reopening. Paper ARMA-95-0217. In *Proceedings of* the *35th U.S. Symposium on Rock Mechanics (USRMS), Reno, Nevada, June 1995*.
6. Desroches, J. & A. Kurkjian. 1999. Applications of Wireline Stress Measurements. Paper SPE-58086,

SPE *Reservoir Evaluation & Engineering* 2(5), 451–461.

7. Desroches, J., E. Peyret, A. Gisolf, A. Wilcox, M. di Giovanni, A. Schram de Jong, S. Sepehri, R. Garrard, S. Giger. 2021. Stress measurement campaigns in scientific deep boreholes – focus on tool and methods. SPWLA-2021-0056. In *SPWLA 62nd Annual Logging Symposium, May 2021.*
8. Haimson, B.C., and F.H. Cornet. 2003, ISRM Suggested Methods for Rock Stress Estimation—Part 3: Hydraulic Fracturing (HF) and/or Hydraulic Testing of Pre-Existing Fractures (HTPF*), International Journal Rock Mechanics and Mining Sciences*, 40(7–8), 1011–1020.
9. Hergert, T., O. Heidbach, K. Reiter, S.B. Giger, and P. Marschall. 2015. Stress field sensitivity analysis in a sedimentary sequence of the Alpine foreland, northern Switzerland, *Solid Earth*, 6, 533–552.
10. Malik, M., C. Jones and E. Boratko. 2016. How can microfracturing improve reservoir management. *Petrophysics* 57(5), 492-507.
11. Mishra, V. K., P. Lywood and C. Ayan. 2011. Application of Wireline Stress Testing for SAGD Caprock Integrity. Paper SPE 149456. In *Proceedings of the Canadian Unconventional Resources Conference, Calgary, Alberta, Canada, November 2011*.
12. Möri, A. and B. Lecampion. 2021. Arrest of a radial hydraulic fracture upon shut-in of the injection. *International J. of Solids and Structure*, 219-220 (2021) 151-165.
13. Nagra TBO BUL 1-1 Final report. 2021a. Nagra Arbeitsbericht. NAB 20-008.
14. Nagra TBO TRU 1-1 Final report. 2021b. Nagra Arbeitsbericht. NAB 20-009.
15. Nelson, E.J., J.J. Meyer, R.R. Hillis and S.D. Mildren. 2005. Transverse drilling-induced tensile fractures in the West Tuna area, Gippsland Basin, Australia: implications for the in-situ stress regime*. International Journal of Rock Mechanics and Mining Sciences*, 42(3), 361-371.
16. Nolte, K.G. 1982. Fracture design considerations based on pressure analysis. Paper SPE-10911 In *Proceedings of the SPE Cotton Valley Symposium, Tyler, Texas, USA, May 1982*.
17. Nolte, K.G. 1988. Application of fracture design based on pressure analysis. Paper SPE-13393, *SPE Production Engineering* 3(1), 31-42.
18. Plahn, S., K.G. Nolte and S. Miska. 1995. A quantitative investigation of the pump-in/flowback test. In *Proceedings of the SPE Annual Technical Conference & Exhibition, Dallas, USA, October 1995*.
19. Povstyanova, M., M. Coscia, P. Van Laer, G. Makarychev, H. Al Marzooqi, K. Leyrer, N. Casson, K. Cig, and J. Desroches. 2018. Stress Testing with Improved Wireline Formation Tester in Low Permeability Unconventional Formation. Paper SPE-193272 In *Proceedings of the Abu Dhabi International Petroleum Exhibition & Conference, Abu Dhabi, UAE, November 2018*.
20. Thiercelin, M., J. Desroches, J., and A. Kurkjian. 1994. Open hole stress tests in shales. Paper SPE 28144 In *Proceedings of the* Rock *Mechanics in Petroleum Engineering, Delft, Netherlands, August 1994.*
21. Thiercelin, M., R. Plumb, J. Desroches, P. Bixenman, J. Jonas and W. Davie. 1996, A New Wireline Tool for In-Situ Stress Measurements, Paper SPE-25906, *SPE Formation Evaluation*, 11(1), 19–25.
22. Wileveau, Y., F.H. Cornet, J. Desroches, and P. Blumling. 2007. Complete in situ stress determination in an argillite sedimentary formation. *Physics and Chemistry of the Earth, Parts A/B/C*, 32(8-14), 866-878.